

Article

Optimization of Very Short Multi-Pump Discrete Raman Amplifiers based on Tellurite Fibers

Gabriel C. Bastida¹ , Helder R. de O. Rocha¹ , Marcelo E. V. Segatto¹ , Carlos E. S. Castellani¹ 

¹Electrical Engineering Department, Federal University of Espírito Santo (UFES), Vitória, ES, Brazil.
gabriel.bastida@edu.ufes.br; helder.rocha@ufes.br; marcelo.segatto@ufes.br; carlos.castellani@ufes.br

Abstract— This paper presents a numerical study and the optimization of very short discrete multi-pump Raman amplifiers using Tellurite-based optical fibers. While most studies about discrete Raman amplifiers usually focus on cases where hundreds of meters of fiber are used, here we consider a multi-pumped Raman amplifier setup with extremely short dimensions, in which the length of the gain media was varied from 2.5 to 30 meters. The optimization process was developed over an broad amplification band from 1520 to 1600 nm, considering a maximum acceptable ripple of 3 dB, and using 2, 3 and 4 pumps with individual powers always below 2.5 W. The results show that it is possible to achieve net gains as high as 10 dB for gain media around 20 meters, and close to 15 dB for 30 meters. These high gains highlight the fact that Tellurite-based optical fibers can be used for the construction of very short and compact broadband amplifiers using just a few pump lasers with modest optical powers.

Index Terms— Discrete Raman amplifier, Stimulated Raman Scattering, Tellurite optical fibers.

I. INTRODUCTION

Raman scattering in fiber optics has played an important role over the last decades in Wavelength Division Multiplexed (WDM) transmission systems, mainly due to its use as Raman fiber amplifiers [1]. This type of amplification offers many advantages in comparison to other conventional amplifiers, such as presenting low noise figures, and allowing a broad and flexible gain bandwidth to be achieved using relatively simple structures [2]. Moreover, such gain bandwidth shaping flexibility in Raman amplifiers have attracted a lot of attention, since simply by using an optimized combination of different pump lasers, regarding its wavelength and optical power, the overlapping of the Raman gain spectrums related with each pump could yield the construction of wide band flat-gain amplifiers, encompassing optical telecommunication systems to operate in the full extent from the S- to the L-band [3], [4].

In addition, in recent decades the continuous growing demand for bandwidth due to the widespread popularity of Internet services has exerted mounting pressure to achieve a better use of the optical window to support information-hungry necessities of our society by improving data-carrying capacity. Among the main proposed solutions for this problem around the C- and L-bands, we can highlight the construction of telecommunication systems based on few-mode fibers [5], the use of multicore fibers [6], or even the simultaneous use of both techniques together on the same fiber [7]. Another possible

solution to help overcome this ever-increasing demand problem is to expand the accessible optical transmission window in order to reach telecommunication systems built on wavelengths up to 2 μm , where silica fibers are not good candidates due to its huge loss when comparing to the 1550 nm band. For this purpose, it is necessary to find new glasses to make optical waveguides, especially with features that differ from fused silica fibers, so that they could allow the construction of linear and nonlinear devices and systems around the 2000 nm band. In this context, the development of high-gain broadband Raman amplifiers in such non-silica glasses is vital towards achieving this type of telecommunication systems. Taking into account this demand, many non-silica glasses have already been developed finding applications in a large variety of nonlinear devices in the mid-infrared (mid-IR) range, based mostly on materials such as tellurite [8], fluoride [9] and chalcogenide [10] glasses. Among those options, tellurite glasses has received special research attention due to the combination of some of its physical, thermal and optical attributes, including thermal and mechanical stability, non-corrosive structure, wide transmission region from 0.5 to 5 μm , high linear and nonlinear refractive indices, high Raman gain coefficients and high earth-rare ions solubility [11], [12], which allows the glass fiber to be doped with different ions and emit light at different wavelengths [13]. Moreover, tellurite fibers have already been proved to be suitable for nonlinear optical applications. As a consequence of its high Raman gain coefficient, around 35 to 50 times higher than that of fused silica [12], tellurite fibers have been used for supercontinuum mid-IR generation [14], fiber Raman lasers [15] and doped-fiber amplifiers [16], for example, in regions that fused silica fibers could not cover. Other important application is its potential use as a gain media for broadband Raman amplifiers applied to telecommunication bands, as demonstrated in [17]. Even though tellurite fibers usually present attenuation levels approximately of 30 dB/km around the 1550 nm band, which are way above what we find in silica fibers, their much higher Raman gains usually can compensate for this disadvantage, especially if we are considering the construction of short length discrete Raman amplifiers.

Wide-band tellurite-based discrete amplifiers have already been demonstrated for bandwidths close to 160 nm using gain media between 200 and 300 meters, by employing a three-stage amplification configuration, composed by two- λ -pumped tellurite fiber Raman amplifier (T-FRA) stages and a two- λ -pumped dispersion compensating fiber Raman amplifier stage set between the T-FRA stages [18]. Despite the net gain achieving a maximum peak of 34.5 dB for a specific wavelength in [18], the obtained ripple was close to 11 dB. In [19], a special care was taken to minimize the ripple and gains as high as 10 dB were achieved maintaining the ripple values around 3 dB, when using 3 pumps and gain media lengths between 100 and 200 meters. In another case, [20] proposed a T-FRA that covered only a narrow amplification band of 47 nm, yielding an average gain above 17 dB while keeping ripple below 0.7 dB but at the cost of cascading two tellurite fibers with a total measurement longer than half a kilometer, pumped by two lasers, as a gain media. Then, considering the expensive costs per meter of tellurite fibers, these reported hundred meters long amplifiers are high-priced setups, which is a disadvantage that makes them less attractive to commercial and laboratory usages. However, it is possible to take advantage of the high nonlinearities and also of the broad two-peak shape of the Raman gain spectrum of tellurite glasses [11], [12] in order to build optimized broadband Raman amplifiers based on extremely short lengths of tellurite fibers as gain media using just a few pump lasers. The use of very short fiber lengths, of approximately a few tens of meters, not only can make such amplifiers much cheaper but equally it can avoid the intense attenuation of this glass allowing high broadband

gains to be achieved even when pump lasers with modest powers.

In this paper, we propose a numerical study focused on the optimization of tellurite-based fiber Raman amplifiers for applications in the 80 nm bandwidth ranging from 1520 to 1600 nm, considering the gain media based on the $\text{TeO}_2 - \text{Bi}_2\text{O}_3 - \text{ZnO} - \text{Na}_2\text{O}$ (TBZN) glass composition, the same fiber material that was used in [19], [21]. While most studies about discrete Raman amplifiers in such fibers focus on cases where hundreds of meters are employed, here we considered multiwavelength pumping Raman amplifiers with extremely short dimensions, in which the gain media was varied from 2.5 to 30 meters. For each length of tellurite fiber, optimization processes were performed considering different scenarios where 2, 3, or 4 pumps were used, and the maximum individual pump powers were always kept below 2.5 W. These amplifiers were optimized using a combination of previously reported analytical and numerical algorithms [22], [23], [24], which provided a fast and reliable process. The final result shows that the high Raman gain coefficient of tellurite-fibers and its broad two-peak shape allows the construction of Raman amplifiers with acceptable average gain and spectral flatness response over a broad bandwidth, keeping it cheaper and more compact than the previously reported tellurite-based fiber Raman amplifiers. In Section 2 the analytical and numerical algorithms models are presented and the technique utilized to perform the optimization is discussed, and the results achieved are reported and discussed in Section 3.

II. SETUP AND OPTIMIZATION TECHNIQUES

The Raman fiber amplifier setup used for this work is illustrated in Fig. 1, where for simulation simplicity we have considered a WDM telecommunication system with 20 signal channels equally distributed over the spectral window ranging from 1520 to 1600 nm and each channel operating with -5 dBm as the input power. The mentioned 1520-1600 nm band was set after a review on the amplification band of related works [18], [19], [20], so deciding to choose a spectral window covered by their amplifiers as a way to allow us to compare our results with the literature. Moreover, using this band is also an opportunity to show that our proposed setup can be a valid alternative to be used as a discrete amplifiers for standard telecommunication systems especially if we are thinking about using few pumps and short fibers, and still achieving high gains and small ripples. All those signals were coupled into a tellurite-based fiber, that was used only as the gain medium of the amplifier. Here, the tellurite fiber data used in the simulations was based on the fiber experimentally demonstrated by Mori *et al.* in [21], also known as TBZN.

This TBZN fiber has reasonably high Raman gain values for frequency shifts between pump and signal for a broadband range from approximately 4-25 THz, where its value is above $25 (\text{W.km})^{-1}$ for almost this entire shift region. Through all this range of frequency shifts, the Raman gain coefficients are at least one order of magnitude higher than that of fused silica [21], but there are two highlighted peaks - the highest peak of $55 (\text{W.km})^{-1}$, related to a frequency shift of 22.2 THz, followed by the second peak of $38.4 (\text{W.km})^{-1}$ for a frequency shift close to 13 THz. These high widespread gain coefficients and the high gain peaks make tellurite fibers useful for optimizing flat wideband Raman amplifiers demanding few pump lasers. Additionally, the fiber attenuation is slightly below 30 dB/km over the 1520-1600 nm window [19], which means that it is unfeasible to use this type of fibers as both transmission medium and gain medium, in the same manner that fused silica fibers are used in distributed amplifiers. On the other hand, however, its very high Raman gain coefficient make it

possible to obtain very high net gains using only few meters of tellurite fibers while avoiding an increased attenuation loss.

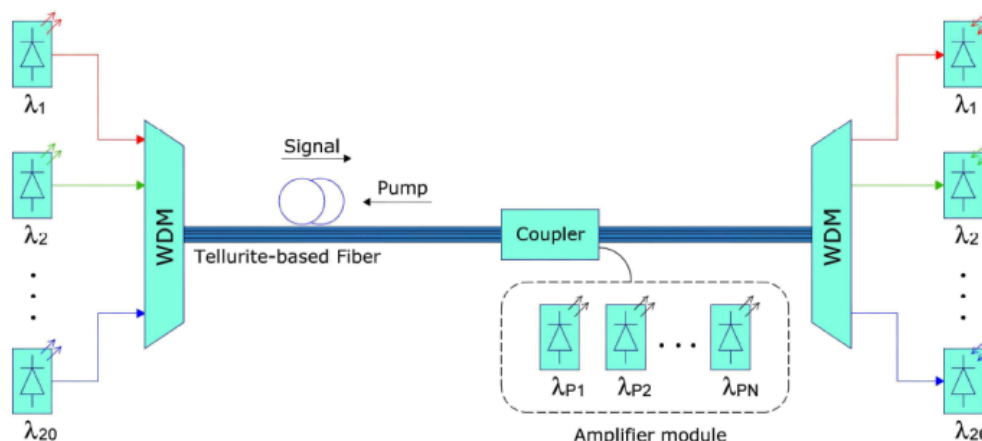
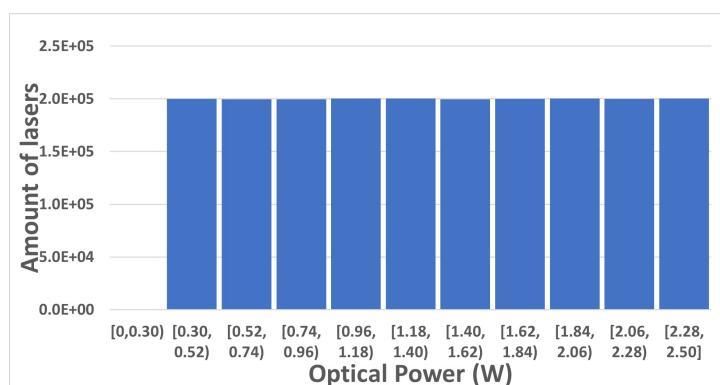


Fig. 1. Generalization of the tellurite-fiber Raman amplifiers setup variables. Extracted from [19].

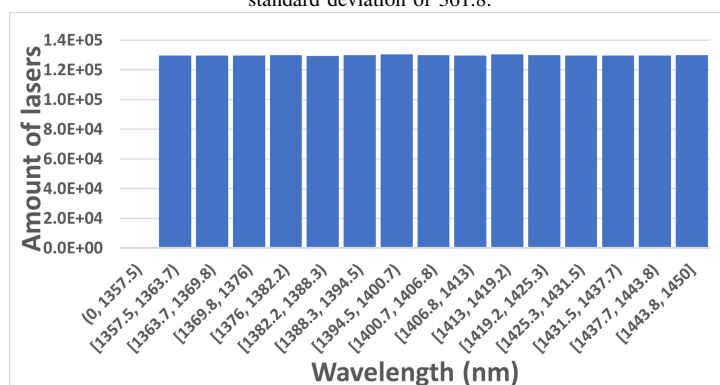
We used a N -counter-propagating pump configuration, in which for the sake of simplicity in the setup we chose to keep $N = 2, 3$ or 4 in order to find the best cost-effectiveness options considering a trade-off between gain media length, individual optical pump power and the amount of pump lasers. We limited N between 2-4 because it was possible to take advantage of the two-peak Raman gain spectra of tellurite to produce great results without the necessity of employing complex pumping systems, keeping our setups as simple and compact as we possibly can. Additionally, according to [25], it is notable that pump systems with more than 4 lasers very often bring only marginal improvements when comparing to a 4 or 3 pump system. For instance, in [21] a seven-pump telluride-based Raman amplifier was projected producing an average gain over its amplification band below 15 dB followed by a ripple above 10 dB. Next, we allowed the pump wavelengths, $\lambda_{p1}, \dots, \lambda_{pN}$, to vary in the range from 1357.5 to 1450 nm; the maximum optical power, P_{max} , was analysed for different cases, varying from 1.0 W to 2.5 W, but always fixing their minimum optical pump power in 300 mW. We considered this range of P_{max} as a strategy to compensate the negative influence of the extreme gain media shortening in the amplifier net gain, since lasers with such optical power levels are much more readily available if compared with long lengths of tellurite fibers, while the minimum optical power was set as a way to ensure a more complete and accurate investigation of the solution-space that is useful to our goals of building a short amplifier using few pumps. Another parameter that was allowed to vary for the optimization process was the tellurite fiber length, L , used as the gain media. Here, the amplifiers simulations were performed considering L varying from 2.5 to 30 meters, with steps of 2.5 meters, in order to find the minimum fiber length necessary to achieve reasonable net gains all over the 80 nm bandwidth for each situation analyzed.

The optimization process was accomplished following two subsequent parts, and each part was based on the use of a different algorithm responsible to find the gain curve obtained for multi-pumped Raman amplifiers, exactly as in [23], [24] where an analytical and a numerical approach are combined in a similar methodology and the results were validated. Table I summarizes the proposed methodology. The first stage, based on the very fast analytical solution from [22], was employed primarily to allow us to exploit very large solution-spaces in a very short computational time. So, this analytical model was used to solve $500 \cdot 10^3$ randomly generated pump configurations for each one of the whole possible

combinations between N pumps - $\lambda_{p1}, \dots, \lambda_{pN}$, limited to a maximum pump optical power of P_{max} and L -meters-long fiber gain media. It took less than an hour to evaluate each of the half-million points iterations. So, considering that we have a consolidated and very fast analytical algorithm that is able to provide accurate solutions in a very short-time, it was not necessary for us to implement a complex meta-heuristics usually associated with numerical solutions of the Raman gain propagation. Our exhaustive search approach allows us to explore a much bigger solution space, therefore avoiding problems of possibly falling into locally optimized solutions, as shown already in [23] and [24]. As an example, in the Fig. 2, it is possible to verify the distribution of the sampled points randomly generated during the optimization process for $N = 4$, $P_{max} = 2.5W$ and $L = 20m$. As one can see in Fig. 2(a) and Fig. 2(b) respectively, the generated samples - each sample consisting of $N = 4$ lasers, so totaling 2.10^6 randomly generated lasers - are equally distributed over their whole range of optical power and wavelength available, as we expected. In the Fig. 2(a), the distribution of the 2.10^6 generated lasers has a mean of 200.10^3 in each column and a standard deviation of only 361.8, while in Fig. 2(b) it has a mean of, approximately, 130.10^3 lasers in each column and a standard deviation of just 287.9.



(a) Distribution of the 500.10^3 randomly generated four-pumped-systems by its optical power. The distribution has a mean of 200.10^3 lasers in each column and standard deviation of 361.8.



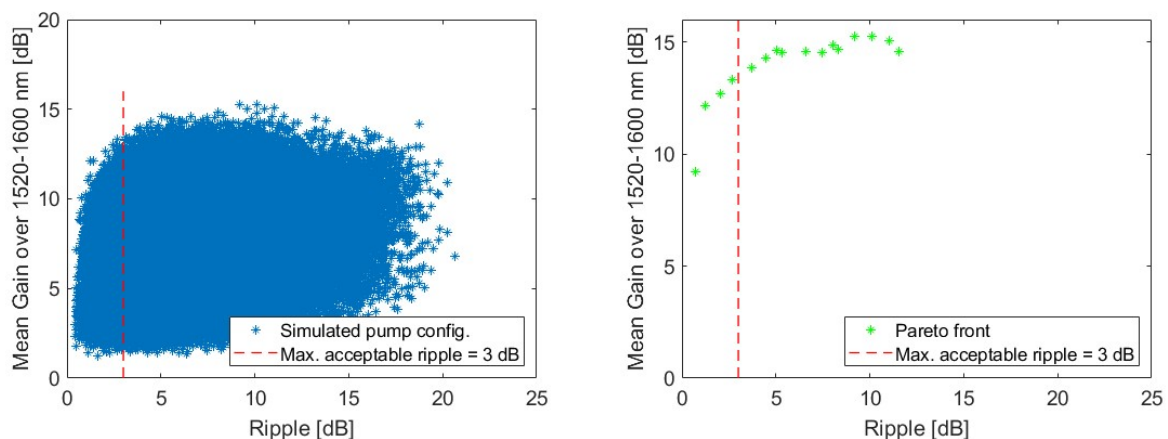
(b) Distribution of the 500.10^3 randomly generated four-pumped-systems by its wavelength. The distribution has a mean of $129.8.10^3$ lasers in each column and standard deviation of 287.9.

Fig. 2. Description of the 500.10^3 randomly generated pump systems for $N = 4$, $P_{max} = 2.5W$ and $L = 20m$.

Afterwards, all these data generated by the analytical solution were processed, looking for the five pump configurations of each iteration that presented the highest gains in the solution-space delimited by a maximum acceptable ripple of 3 dB, as depicted on Fig. 3, where it is possible to see an example of the evaluated solution's cloud generated for the optimization when $N = 2$, $P_{max} = 2.5W$ and $L = 30m$. In the Fig. 3(a), the drawn dashed red line is highlighting the solution's region delimited by

the maximum acceptable ripple, which in our case is 3 dB. In addition, in order to clarify the search performed on the fourth step of Table I, Fig. 3(b) is showing the Pareto's front of the previously cited cloud, that was used to support us to find the five best solutions within the acceptable ripple space. Also, it is important to mention that our proposed optimization method always allow us to easily generate a very accurate Pareto front curve, which can be very useful when deciding about what should be the acceptable ripple and gain space for each different type of setup.

On the second stage, in order to improve the precision of the final results, these sets of five configurations were used as inputs for a very accurate numerical solution and re-simulated, similarly as in [23], [24]. In sequence, due to the difference in the gain and ripple provided by the numerical solution from the analytical one, the final results were listed in descending order of gain values and again filtered by maximum ripple of 3 dB. Finally, pump configurations related with the highest gain were selected for each one of the simulated combinations. In general, the analytical results were in good agreement with the numerical solutions. For the two and three-pump systems, we found error margins always lower than 10%, and for systems pumped by four lasers the error margins could always be kept below 20%. Nevertheless, it is important to highlight that these small inaccuracies are not observed on the final results presented in this paper, since at the end of the optimization process we always employ the more accurate numerical solution on its validation.



(a) Example of the solution cloud generated by the analytical algorithm used on Step 3 from Table I, with the maximum acceptable ripple line on 3 dB.

(b) Example of the Pareto's front used on Step 4 from Table I, highlighting the highest gain for multiple ripple levels, with the maximum acceptable ripple line on 3 dB.

Fig. 3. Results of the 500.10^3 pump configurations randomly generated and evaluated by the analytical algorithm during the optimization for $N = 2$, $P_{max} = 2.5W$ and $L = 30m$.

III. RESULTS

A. Two-counter-propagating pump systems

For the case of the Raman amplifiers using only two pumps, the highest average gain achieved and its respective gain ripple level reached for each optimized amplifier setup analyzed as function of tellurite fiber length, L , and maximum optical power, P_{max} , are exposed in Fig. 4 and in Fig. 5. For both Figures, each dot on the graphs is representing an optimized setup. As one can notice, in Fig. 4 average gain increases almost linearly as a function of fiber length, but with wider angular coefficient for higher P_{max} values, as expected. Moreover, Fig. 5 highlights the fact that the ripple levels are always kept below the 3 dB threshold, as defined by our optimization process explained on Section

TABLE I. SCHEMATIC ALGORITHM DESCRIBING THE OPTIMIZATION METHODOLOGY ADOPTED.

Step 1	Define amplifier optimization inputs: amplification bandwidth, N , λ_{p1} , ..., λ_{pN} , P_{max} , L ;
Step 2	Define pump wavelength, maximum optical power and tellurite fiber length ranges and amount of pumps to be investigated;
Step 3	Run the analytical solution algorithm to generate and solve $500 \cdot 10^3$ random pump configurations for all possible amplifier configurations;
Step 4	Filter, by maximum acceptable ripple and gain, the five best configurations for each amplifier;
Step 5	Run the accurate numerical algorithm with the chosen configurations to improve solution precision;
Step 6	Filter the results by acceptable ripple and pick the configuration with the highest gain for each amplifier;

2. It is important to mention that only for these two-pump systems, the optimization process was not computed for setups based on pumps limited to a maximum optical power of 1 W, due to the fact that very low average gains were always obtained, making the amplifiers unfeasible in practice.

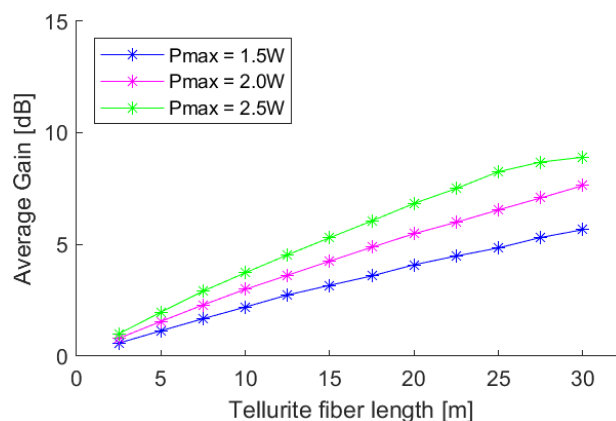


Fig. 4. Average net gain (stars) as function of tellurite fiber length for optimized amplifiers systems powered by two pumps and maximum optical pump power, P_{max} , equal 1.5 W (blue), 2.0 W (magenta) and 2.5 W (green).

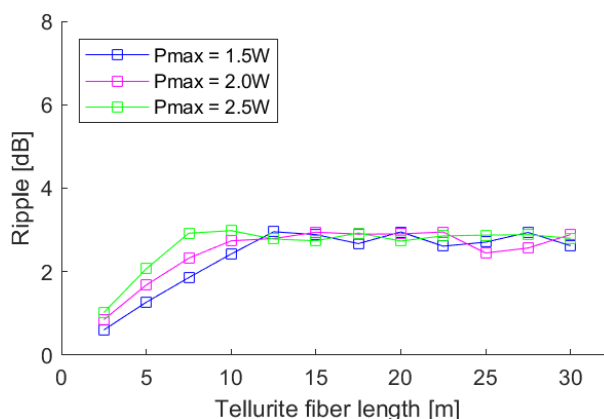


Fig. 5. Ripple level (squares) as function of tellurite fiber length for optimized amplifiers systems powered by two pumps and maximum optical pump power, P_{max} , equal 1.5 W (blue), 2.0 W (magenta) and 2.5 W (green).

In sequence, we selected three optimized amplifiers in order to show their spectral performance over the 1520-1600 nm window, and to allow us to better evaluate the individual net gain over the 20 WDM



channels established. Then, Fig. 6 shows the net gain as function of wavelength over the 80 nm band for fiber lengths of 10, 20 and 30 meters, respectively, considering a P_{max} equal 2.5 W. As can be noticed, all three setups are presenting flatness gain over its covered bandwidth and an increasing gain level according to the increases in tellurite fiber length. Additionally, we can see that for amplifiers using only two pumps 10 meters of fiber is not enough to provide high average gains even when considering 2.5 W pump powers. However, this result shows that when using 30 meters of gain fiber an amplifier with nearly 9 dB of average net gain can be built while keeping the ripple at a low value. Table II summarises the description of the optimized two-pumped systems used for Fig. 6.

TABLE II. DESCRIPTION OF PUMP LASERS USED ON FIG. 6 SYSTEMS

Fiber Length [m]	$\lambda_{p1}, \lambda_{p2}$ [nm]	P_{p1}, P_{p2} [W]	Average Gain [dB]	Ripple [dB]
10	1412.0, 1425.8	2.485, 2.422	3.719	2.984
20	1389.6, 1422.0	2.500, 2.490	6.828	2.734
30	1398.4, 1434.7	2.432, 2.232	8.901	2.801

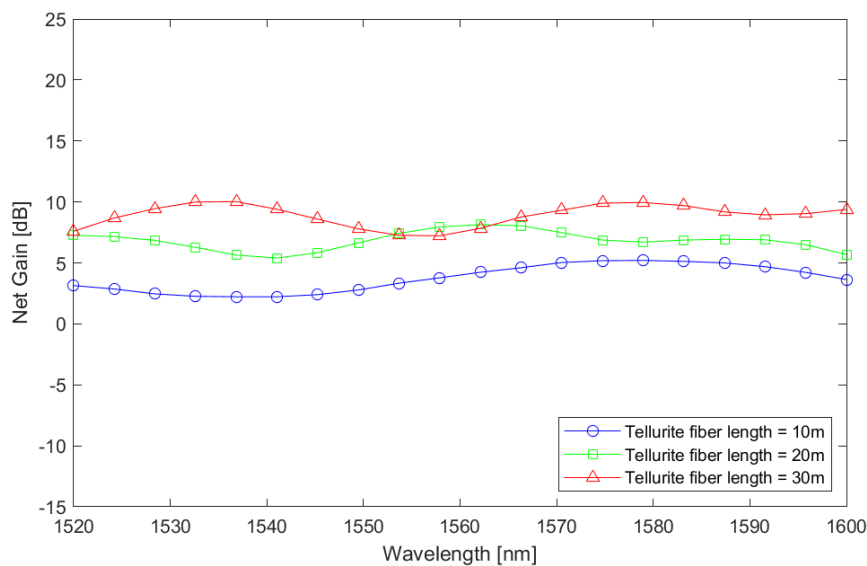


Fig. 6. Net gain as function of wavelength over the 1520-1600 nm spectral window for optimized two-pumped amplifiers using gain media length of 10 meters (in blue), 20 meters (in green) and 30 meters (in red). P_{max} was set at 2.5 W.

B. Three-counter-propagating pump systems

The average net gain and ripple as a function of gain media length and P_{max} for the three-pumped amplifier setups are depicted in Fig. 7 and Fig. 8, respectively. Differently from the amplifier setups using two pumps, the results achieved for the optimized amplifiers considering P_{max} limited to 1.0 W are relevant, since they provide average gains as high as most of the ones obtained for two pump systems, even demanding shorter fiber lengths and lower pump powers. As shown in Fig. 7, average gains higher than 7.5 dB were achieved for fiber lengths greater or equal to 20 meters, for P_{max} of 2.0 and 2.5 W, while still keeping the ripple levels below 3 dB, as seen in Fig. 8. Moreover, for amplifiers based on gain media between 25 and 30 meters and pumped with optical power of up to 2.5 W, it should be pointed that it was possible to achieve net gains slightly close to 12 dB while maintaining gain ripple around 2.5 dB. Notably, the presented gain levels are proportional to the gain media length, but differently from the obtained result for the two pump systems, here it is possible to notice that the



amplifier gains for some cases start to saturate for fiber lengths longer than 20 meters, specially when considering the system using P_{max} of up to 2.5 W.

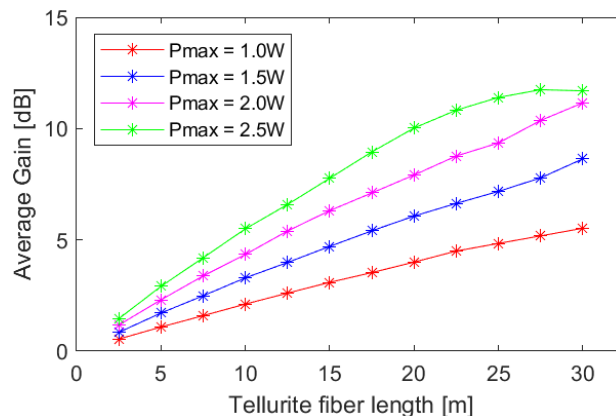


Fig. 7. Average net gain (stars) as function of tellurite fiber length for optimized amplifiers systems powered by three pumps and maximum optical pump power, P_{max} , equal 1.0 W (red), 1.5 W (blue), 2.0 W (magenta) and 2.5 W (green).

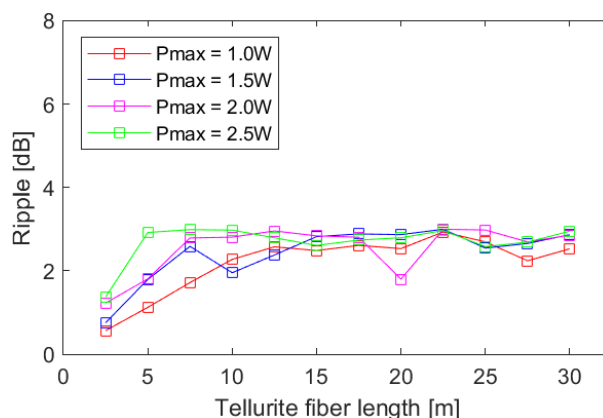


Fig. 8. Ripple level (squares) as function of tellurite fiber length for optimized amplifiers systems powered by three pumps and maximum optical pump power, P_{max} , equal 1.0 W (red), 1.5 W (blue), 2.0 W (magenta) and 2.5 W (green).

In addition, three optimized amplifier solutions were chosen in order to have a deeper analysis of their performance. In Fig. 9 we can see their individual net gain as a function of the 20-WDM-channels wavelengths. For the results exhibited in Fig. 9, we chose the optimized setups shown in Fig. 7 for gain media lengths of 10, 20 and 30 meters, considering 2.5 W as P_{max} . It is easy to notice that all three setups present a very flat gain curve, confirming our optimization goal to not allow ripple levels above 3 dB. Table III summarises the description of the optimized three pump systems simulated for Fig. 9.

TABLE III. DESCRIPTION OF PUMP LASERS USED ON FIG. 9 SYSTEMS

Fiber Length [m]	$\lambda_{p1}, \lambda_{p2}, \lambda_{p3}$ [nm]	P_{p1}, P_{p2}, P_{p3} [W]	Average Gain [dB]	Ripple [dB]
10	1403.2, 1415.3, 1432.1	2.452, 2.379, 2.496	5.494	2.978
20	1384.5, 1397.3, 1429.1	2.481, 2.468, 2.494	10.02	2.795
30	1387.6, 1398.7, 1429.3	2.396, 1.879, 1.808	11.69	2.952

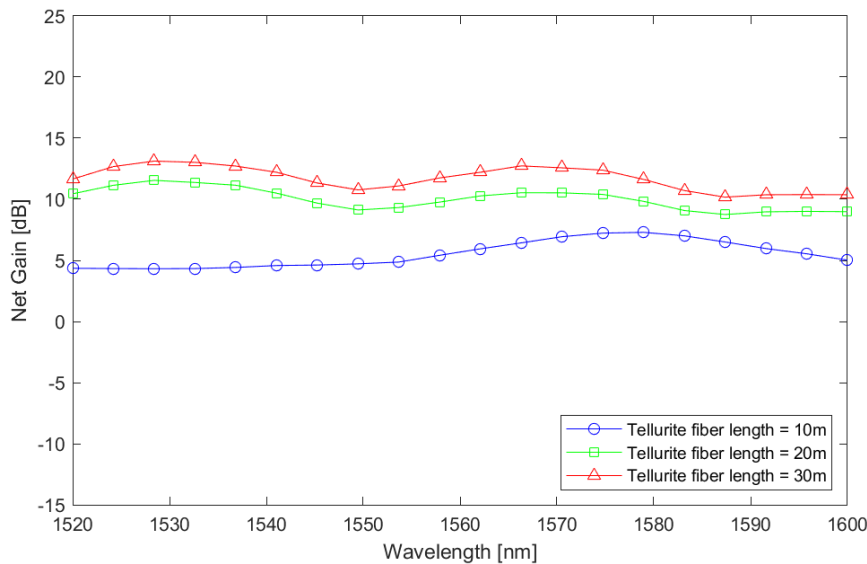


Fig. 9. Net gain as function of wavelength over the 1520-1600 nm spectral window for optimized three-pumped amplifiers using gain media length of 10 meters (in blue), 20 meters (in green) and 30 meters (in red). P_{max} was set at 2.5 W.

C. Four-counter-propagating pump systems

For systems using four pumps, the results of the optimization process are exhibited in Fig. 10 and Fig. 11, where one can see, respectively, the average net gains and ripple levels as a function of the tellurite fiber length and the maximum available optical pumps power, P_{max} . According to Fig. 10, gains greater than 7.5 dB were achieved employing shorter gain media than for three pumps systems. Furthermore, the high values of gain reached using four pumps can easily reach values higher than 10 dB and, in the best scenario, close to 15 dB while keeping ripple values close to only 2 dB, such as when using 30 meters of tellurite fiber and 2.5 W as P_{max} .

Additionally, it is important to note in Fig. 11 that four of the optimized amplifiers obtained presented ripple levels slightly above 3 dB. Despite the main goal to keep ripple below 3 dB, when using four pumps, specially at higher pump powers, the analytical and the numerical solution start to diverge slightly since there is no pump depletion included in the analytical model, which made solutions with ripples close to 3 dB jump to higher values when testing them on a more accurate numerical model. Nevertheless, apart from the case where a 25 meters tellurite fiber was used under P_{max} of 2.5 W in which the ripple was around 4.4 dB, for all other cases we had a maximum ripple of only 3.6 dB, very close to what was designed by the optimization goals and simulated with the analytical model.

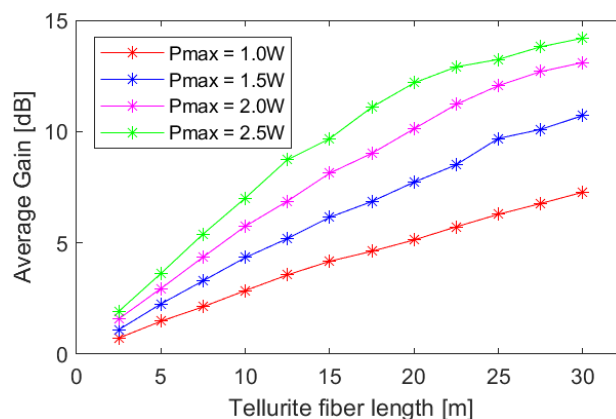


Fig. 10. Average net gain (stars) as function of tellurite fiber length for optimized amplifiers systems powered by four pumps and maximum optical pump power, P_{max} , equal 1.0 W (red), 1.5 W (blue), 2.0 W (magenta) and 2.5 W (green).

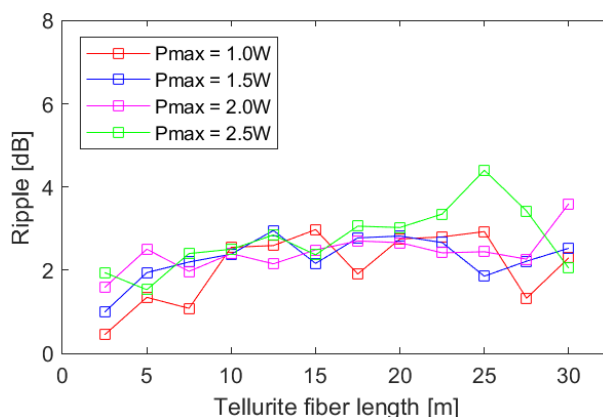


Fig. 11. Ripple level (squares) as function of tellurite fiber length for optimized amplifiers systems powered by four pumps and maximum optical pump power, P_{max} , equal 1.0 W (red), 1.5 W (blue), 2.0 W (magenta) and 2.5 W (green).

It is possible to compare the average gains shown in Fig. 4, Fig. 7 and Fig. 10 and realize that the optimized Raman amplifiers pumped by four pumps present the highest net gain results, as expected. Furthermore, for the four-pump systems it is easy to reach a wider variety of net gains that demand less tellurite fiber length than in the previous setups. Additionally, these results show that a simple and very short tellurite-based Raman amplifiers can be used in telecommunication systems and laboratories to provide high gains in very compact devices. Again, as discussed for the three-pump amplifiers, their net gains become less sensitive with increases in gain media length approximately after it reaches 20 meters.

Again we chose three of the optimized amplifiers to show their detailed spectral performance over the 1520-1600 nm window. Fig. 12 shows the net gain as function of wavelength for each of the 20 WDM channels. The curves shown in Fig. 12 were obtained from the amplifiers optimized using P_{max} equal to 2.5 W and tellurite fiber lengths of 10, 20 and 30 meters, respectively. According to Fig. 12, it is notable that the four-pump amplifiers present better flatness than the previous ones presented on Fig. 6 and Fig. 9, which is expected when you have a bigger combination of pump powers and wavelengths. Table IV summarise the description of the optimized four-pumped systems simulated for Fig. 12.

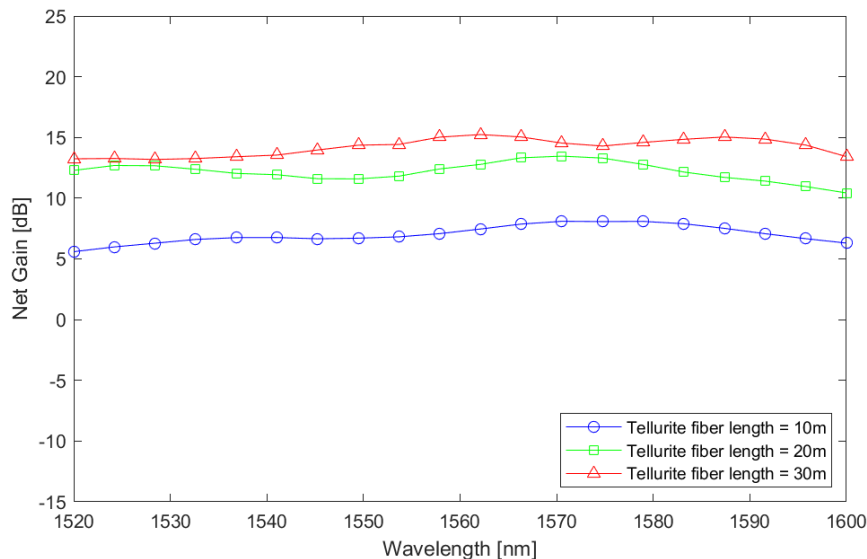


Fig. 12. Net gain as function of wavelength over the 1520-1600 nm spectral window for optimized four-pumped amplifiers using gain media length of 10 meters (in blue), 20 meters (in green) and 30 meters (in red). P_{max} was set at 2.5 W.

TABLE IV. DESCRIPTION OF PUMP LASERS USED ON FIG. 12 SYSTEMS

Fiber Length [m]	$\lambda_{p1}, \lambda_{p2}, \lambda_{p3}, \lambda_{p4}$ [nm]	$P_{p1}, P_{p2}, P_{p3}, P_{p4}$ [W]	Average Gain [dB]	Ripple [dB]
10	1400.0, 1401.1, 1420.6, 1437.7	2.333, 2.323, 2.446, 2.427	7.015	2.505
20	1387.1, 1387.2, 1406.1, 1427.5	2.444, 2.049, 1.972, 2.441	12.19	2.999
30	1374.0, 1402.4, 1420.4, 1447.5	2.299, 2.426, 2.301, 0.680	14.20	2.049

IV. CONCLUSIONS

This paper shows an optimization process applied to discrete multi-pump Raman amplifiers based on very short tellurite fibers. Using an analytical method previously reported as a preliminary solution, it was possible to inspect half a million Raman amplification's setups in each solution-space within a short processing time and, then, to filter the best configurations of pump lasers that lead to the highest gains keeping the ripple limited to 3 dB. Optimizations were performed considering the tellurite fiber length, amount of pumps and maximum optical pump powers available as variable parameters. The performance of the filtered pump configurations were more accurately evaluated using a more precise and complete numerical solution method.

The results obtained here show that the high Raman gain coefficients of tellurite-based glasses, and also its broad multi-peak shape, make those fibers an interesting gain media solution for constructing very compact discrete Raman amplifiers, with fiber lengths on the range of a few tens of meters. Here we found optimized broadband and low-ripple amplifier configurations employing much smaller lengths of tellurite fiber than previously reported, reaching gain levels of up to 15 dB over a bandwidth of 80 nm using not more than 4 pumps. It is important to emphasize that the results presented along this paper were obtained considering an ideal scenario, in which no commercial restriction of wavelength or optical power were imposed for our pump lasers. However, considering that nowadays there is a wide range of lasers that operate over the 1360-1450 nm wavelength window, and the possibility of implementing new ones based on nonlinear effects such as cascaded Raman lasers, it should not be a hard task to find pump lasers similar with the ones proposed above. Small deviation on pump wavelength or optical power should not cause major changes on the amplifier gain profile.

ACKNOWLEDGMENTS

Authors would like to thank and acknowledge funding received from Fundação de Amparo à Pesquisa do Espírito Santo (FAPES), Project "Suporte à Pesquisa e à Inovação: Desenvolvimento de Abordagem de Sistemas", and FAPES-2022-71JG6, FAPES-2021-WMR44, FAPES- 2022-BWBR2; and from Conselho Nacional de Desenvolvimento Científico e Tecnológico (CNPq), CNPq-309737/2021-4, for the development of this research.

REFERENCES

- [1] G. Agrawal, *Nonlinear fiber optics*. Academic Press, San Diego, 2013.
- [2] C. Headley and G. P. Agrawal, *Raman amplification in fiber optical communication systems*. Academic Press, San Diego, 2005.
- [3] U. C. de Moura, M. A. Iqbal, M. Kamalian, L. Krzaczanowicz, and *et al*, "Multi-Band Programmable Gain Raman Amplifier," *Journal of Lightwave Technology*, vol. 39, pp. 429–438, 2021.
- [4] Y. V. Krutin, A. V. Korchak, M. Reznikov, and G. Felinskyi, "Modeling of multiwave pumped fiber raman amplifier for c+l telecommunication windows," in *2020 IEEE 40th International Conference on Electronics and Nanotechnology (ELNANO)*, pp. 319–322, 2020.
- [5] D. J. Richardson, J. M. Fini, and L. E. Nelson, "Space-division multiplexing in optical fibres," *Nature Photonics*, vol. 7, pp. 354–362, 2013.
- [6] K. Saitoh and S. Matsuo, "Multicore Fiber Technology," *Journal of Lightwave Technology*, vol. 34, pp. 55–66, 2016.
- [7] R. G. H. V. Uden, R. A. Correa, E. A. Lopez, F. M. Huijskens, and *et al*, "Ultra-high-density spatial division multiplexing with a few-mode multicore fibre," *Nature Photonics*, vol. 8, pp. 865–870, 2014.
- [8] X. Feng, J. Shi, M. Segura, N. M. White, and *et al*, "Halo-tellurite glass fiber with low OH content for 2-5 μm mid-infrared nonlinear applications," *Optics Express*, vol. 21, pp. 18 949–18 954, 2013.
- [9] V. Fortin, M. Bernier, S. T. Bah, and R. Vallée, "30 W fluoride glass all-fiber laser at 2.94 μm ," *Optics Letters*, vol. 40, pp. 2882–2885, 2015.
- [10] J.-L. Adam, L. Calvez, J. Trolès, and V. Nazabal, "Chalcogenide Glasses for Infrared Photonics," *International Journal of Applied Glass Science*, vol. 6, pp. 287–294, 2015.
- [11] A. Lin, A. Zhang, E. J. Bushong, and J. Toulouse, "Solid-core tellurite glass fiber for infrared and nonlinear applications," *Optics Express*, vol. 17, pp. 16 716–16 721, 2009.
- [12] N. Manikandan, A. Rysanyanskiy, and J. Toulouse, "Thermal and optical properties of TeO₂-ZnO-BaO glasses," *Journal of Non-Crystalline Solids*, vol. 358, pp. 947–951, 2012.
- [13] S. Fu, X. Zhu, J. Wang, J. Wu, and *et al*, "L-Band Wavelength-Tunable Er³⁺-Doped Tellurite Fiber Lasers," *Journal of Lightwave Technology*, vol. 38, pp. 1435–1438, 2020.
- [14] H. Shi, X. Feng, F. Tan, P. Wang, and P. Wang, "Multi-watt mid-infrared supercontinuum generated from a dehydrated large-core tellurite glass fiber," *Optical Materials Express*, vol. 6, pp. 3967–3976, 2016.
- [15] G. Zhu, L. Geng, X. Zhu, L. Li, and *et al*, "Towards ten-watt-level 3-5 μm Raman lasers using tellurite fiber," *Optics Express*, vol. 23, pp. 7559–7573, 2015.
- [16] S. V. Muravyev, E. A. Anashkina, A. V. Andrianov, V. V. Dorofeev, and *et al*, "Dual-band Tm³⁺-doped tellurite fiber amplifier and laser at 1.9 μm and 2.3 μm ," *Scientific Reports*, vol. 8, pp. 1–13, 2018.
- [17] G. Qin, R. Jose, and Y. Ohishi, "Design of Ultimate Gain-Flattened O-, E-, and S+ C+ L Ultrabroadband Fiber Amplifiers Using a New Fiber Raman Gain Medium," *Journal of Lightwave Technology*, vol. 25, pp. 2727–2738, 2007.
- [18] H. Masuda, A. Mori, K. Shikano, and M. Shimizu, "Design and spectral characteristics of gain-flattened tellurite-based fiber Raman amplifiers," *Journal of Lightwave Technology*, vol. 24, pp. 504–515, 2006.
- [19] G. D. de Andrade, H. R. de O. Rocha, M. E. V. Segatto, M. J. Pontes, and C. E. S. Castellani, "Study and Optimization of Raman Amplifiers in Tellurite-Based Optical Fibers for Wide-Band Telecommunication Systems," *Journal of Microwaves, Optoelectronics and Electromagnetic Applications*, vol. 18, pp. 219–226, 2019.
- [20] J. Gong, Y. Zhao, and X. Zuo, "Gain-flattened tellurite-based fiber Raman amplifiers," *The Journal of China Universities of Posts and Telecommunications*, vol. 20, pp. 143–146, 2013.
- [21] A. Mori, H. Masuda, K. Shikano, and M. Shimizu, "Ultra-wide-band tellurite-based fiber raman amplifier," *Journal of Lightwave Technology*, vol. 21, pp. 1300–1306, 2003.

- [22] S. P. N. Cani, L. de Calazans Calmon, M. J. Pontes, M. R. N. Ribeiro, M. E. V. Segatto, and A. V. T. Cartaxo, “An Analytical Approximated Solution for the Gain of Broadband Raman Amplifiers With Multiple Counter-Pumps,” *Journal of Lightwave Technology*, vol. 27, pp. 944–951, 2009.
- [23] C. E. S. Castellani, S. P. N. Cani, M. E. V. Segatto, M. J. Pontes, and M. A. Romero, “Design methodology for multi-pumped discrete Raman amplifiers: case-study employing photonic crystal fibers,” *Optics Express*, vol. 17, pp. 14 121–14 131, 2009.
- [24] C. E. S. Castellani, S. P. N. Cani, M. E. V. Segatto, M. J. Pontes, and M. A. Romero., “Numerical comparison between conventional dispersion compensating fibers and photonic crystal fibers as lumped Raman amplifiers,” *Optics Express*, vol. 17, pp. 23 169–23 180, 2009.
- [25] H. R. de O. Rocha, M. O. L. Benincá, C. E. S. Castellani, M. J. Pontes, M. E. V. Segatto, and J. A. L. Silva, “Performance analysis and comparison of multipump Raman and hybrid erbium-doped fiber amplifier + Raman amplifiers using nondominated sorting genetic algorithm optimization,” *Optical Engineering*, vol. 55, p. 086103, 2016.